ν(C1O1), ν(C2O2), and $\nu(CF_2)$ motions. The band i'' is a valence angle bending motion in the CF_3 end groups, $\alpha(CF_3)$.

The absorptions in the observed copolymer spectrum are assigned as follows: the C-C stretching frequency in the PPFEO calculated spectrum has the highest frequency and also one of weakest intensities; therefore, the weak features marked a'' are assigned to the ν(CC) modes in the propylene oxide unit of the copolymer. Somewhat lower in frequency but of stronger intensity is the CF stretching mode of the CF_2 unit in PPFF; the unresolved but detectable feature marked a' is thus assigned to the $\nu(CF_2)$ of the $-CF_2-O-$ monomeric unit. The broad feature branded c'', d'', and d' is most likely a convolution of the stretches from the CF_2 units in the propylene oxide group and bands due to coupled motions of stretching modes in the CF_2 and C-O groups in both the formaldehyde and propylene oxide monomeric units. The bands marked e'' and e' are both due to C-O stretches which are very intense; e'' has a higher frequency and is assigned to the ν(CO) in CF_2-O while the lower frequency band is assigned to the propylene oxide unit. The absorptions, referred to as f'' and f', are most likely motions due to coupled stretches within the propylene oxide and formaldehyde monomeric units, respectively. Those are the lower frequencies assigned to valence angle bending motions; g' and h' are assigned to the formaldehyde unit while i'' is assigned to the propylene unit.

Registry No. PPFEO (homopolymer), 26591-06-0; PPFEO (SRU), 32107-75-8; PPFPO (homopolymer), 25038-02-2; PPFPO (homopolymer), 35038-02-2; PPFPO (SRU), 62253-59-2; CF_3OCF_3, 1479-49-8; $CF_3CF_2OCF_2CF_3$, 358-21-4; $CF_3CF_2OCF_3$, 665-16-7; $CF_2(OCF_3)_2$, 53772-78-4; $CF_3O(CF_2)_2OCF_3$, 378-11-0; $CF_3OCF(CF_3)CF_2OCF_3$, 95842-02-7.

Carbon Dioxide Activation by Cobalt(I) Macrocycles: Factors Affecting CO_2 and CO Binding

Etsuko Fujita,* Carol Creutz,* Norman Sutin, and David J. Szalda[1]

Contribution from the Chemistry Department, Brookhaven National Laboratory, Upton, New York 11973. *Received April 26, 1990*

Abstract: The cobalt(I) complexes of several 14-membered tetraazamacrocycles were prepared in CH_3CN by either electrochemical or sodium amalgam reduction. The electronic absorption spectra and other physical properties of the Co^I, Co^I-CO_2 and Co^I-CO complexes are reported. The CO_2 and CO binding constants were determined by spectroscopic and/or electrochemical methods. The binding constants range from 5×10^4 to $\geq 3 \times 10^8$ M^{-1} for CO and from ≤ 0.5 to $> 10^6$ M^{-1} for CO_2 at 25 °C. Both binding constants increase as the $CoL^{2+/+}$ reduction potentials (which range from −0.34 to −1.65 V vs SCE in CH_3CN) become more negative. Thus charge transfer from Co^I to CO_2 or CO is an important factor in stabilizing these adducts. However, hydrogen-bonding interactions between the bound CO_2 and amine macrocycle N-H protons may serve to additionally stabilize the adduct in some cases, while steric repulsion by the macrocycle methyl groups may destabilize the adducts, depending upon the complex. The equilibrium ratios of N-meso and N-rac isomers of (5,7,7,12,14,14-hexamethyl-1,4,8,11-tetraazacyclotetradeca-4,11-diene cobalt(I) and -(II) complexes were determined by ^1H NMR; the N-rac isomers of both predominate in CD_3CN at room temperature. The crystal and molecular structure of the perchlorate salt of (3,5,7,7,10,12,14,14-octamethyl-1,4,8,11-tetraazacyclotetradeca-4,11-diene cobalt(I) was determined from single-crystal X-ray diffraction data collected with use of Mo Kα radiation. Crystallographic data: space group $P\bar{1}$ with $a = 8.433$ (2) Å, $b = 18.333$ (4) Å, $c = 7.257$ (2) Å, $\alpha = 100.22$ (2)°, $\beta = 91.29$ (2)°, $\gamma = 87.68$ (2)°, $V = 1103$ (1) Å^3, $Z = 2$ ($R = 0.085$, $R_w = 0.105$). The two square-planar cobalt atoms in the asymmetric unit are situated on crystallographic inversion centers.

Introduction

Although there has been intense interest[2-6] in the electrochemical and photochemical activation of carbon dioxide promoted by transition-metal complexes, only a few detailed mechanistic studies of CO_2 binding to metal complexes have been published. Since Curtis' template synthesis of the $Ni^{II}L_5^{2+}$ (L_5 = 5,7,7,12,14,14-hexamethyl-1,4,8,11-tetraazacyclotetradeca-4,11-diene) complex,[7] many 14-membered tetraazamacrocyclic complexes have shown interesting properties, especially as catalysts for H_2O[8] and CO_2[9,10] reduction. Fisher and Eisenberg[9] reported the electrocatalytic activity of the cobalt(II) and nickel(II) macrocycles in CO_2 reduction in acetonitrile-water mixtures. Gangi and Durand[11] used differential pulse polarography to characterize the reversible binding of CO_2 to $Co^IL_5^+$ ($K_{CO_2} = 7 \times 10^4$ M^{-1}) in dimethyl sulfoxide. We have investigated the reversible binding of CO_2, CO, and H^+ to *N-rac*-$Co^IL_5^+$ in H_2O[12] and CH_3CN,[10,12c] and reversible binding of CO_2 to a series of cobalt(I) macrocycles in DMSO has recently been reported.[13] We have also studied a CO_2 reduction pathway involving two cobalt

(1) Permanent address: Department of Natural Sciences, Baruch College, Manhattan, NY 10010.

(2) Recent reviews: (a) Creutz, C. In *Electrochemical and Electrocatalytic Reduction of Carbon Dioxide*; Sullivan, B. P., Ed.; Elsevier: Amsterdam, in press. (b) Walther, D. *Coord. Chem. Rev.* **1987**, *79*, 135. (c) Ayers, W. M., Ed. *Catalytic Activation of Carbon Dioxide*; ACS Symp. Ser.; American Chemical Society: Washington, D.C., 1988. (d) Behr, A. *Carbon Dioxide Activation by Metal Complexes*; VCH: Weinheim, 1988. (e) Braunstein, D.; Matt, D.; Nobel, D. *Chem. Rev.* **1988**, *88*, 747. (f) Kolomnikov, I. S.; Lysak, T. V.; Rusakov, S. L.; Kharitonov, Y. Y. *Russ. Chem. Rev.* **1988**, *57*, 406. (g) Behr, A. *Angew. Chem., Int. Engl. Ed.* **1988**, *27*, 661. (h) Collin, J. P.; Sauvage, J. P. *Coord. Chem. Rev.* **1989**, *93*, 245.

(3) Recent studies of CO_2 electrochemical reduction promoted by transition-metal complexes: (a) Bruce, M. R. M.; Megehee, E.; Sullivan, B. P.; Thorp, H.; O'Toole, T. R.; Downard, A.; Meyer, T. J. *Organometallics* **1988**, *7*, 238. (b) Bolinger, C. M.; Story, N.; Sullivan, B. P.; Meyer, T. J. *Inorg. Chem.* **1988**, *27*, 4582. (c) Ishida, H.; Tanaka, K.; Tanaka, T. *Chem. Lett.* **1988**, 339. (d) Grunewald, G.; Drago, R. S. *J. Chem. Soc., Chem. Commun.* **1988**, 1206. (e) Kim, J. J.; Summers, D. P.; Frese, K. W. *J. Electroanal. Chem.* **1988**, *245*, 223. (f) Corrigan, D.; Weaver, M. J. *J. Electroanal. Chem.* **1988**, *241*, 143. (g) Hammouche, M.; Lexa, D.; Savéant, J. M.; Momenteau, M. *J. Electroanal. Chem.* **1988**, *249*, 347. (h) Tanaka, K.; Miyamoto, H.; Tanaka, T. *Chem. Lett.* **1988**, 2033. (i) Frese, K. W.; Summers, D. P.; Cinibulk, M. *J. Electrochem. Soc.* **1988**, *135*, 264. (j) Arai, G.; Harashina, T.; Yasumori, I. *Chem. Lett.* **1989**, 1215. (k) Tanaka, K.; Matsui, T.; Tanaka, T. *J. Am. Chem. Soc.* **1989**, *111*, 3765. (l) Azuma, M.; Hashimoto, K.; Hiramoto, M.; Watanabe, M.; Sakata, T. *J. Electroanal. Chem.* **1989**, *260*, 441. (m) Sugiura, K.; Kuwabata, S.; Yoneyama, H. *J. Am. Chem. Soc.* **1989**, *111*, 2361. (n) Garnier, L.; Rollin, Y.; Périchon, J. *New J. Chem.* **1989**, *13*, 53.

0002-7863/91/1513-343$02.50/0

centers and observed the formation of a binuclear species containing the Co–C(OH)–O–Co moiety during the slow decomposition of $Co^{I}L_5CO_2^+$ to $Co^{II}L_5^{2+}$, CO, H_2, HCO_2^-, and HCO_3^- in CH_3CN.[10]

We recently extended our work to other 14-membered cobalt macrocycles in order to investigate the factors governing CO_2 and CO binding and the reactivities of the CO_2 complexes. The Co(II) and Co(III) complexes have been characterized by many groups and have several advantageous properties:[14-22] large variation of $Co^{II/I}$ reduction potentials, reasonably high solubility in water and organic solvents, and relatively fixed ligand geometry with some variation in the steric effects of methyl groups and amine hydrogens. In the case of L_5, for which N-rac and N-meso isomers have been identified,[20] we have been able to explore the role of ligand isomerism.

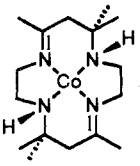

rac-L_5

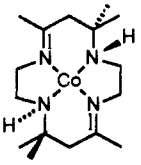

meso-L_5

Here we report the properties of the $Co^{I}L^+$, $Co^{I}L–CO_2^+$, and $Co^{I}L–CO^+$ complexes and the results of our studies of the CO and CO_2 binding equilibria. The abbreviations and structures of the macrocycles used are shown in Chart I.

Chart I

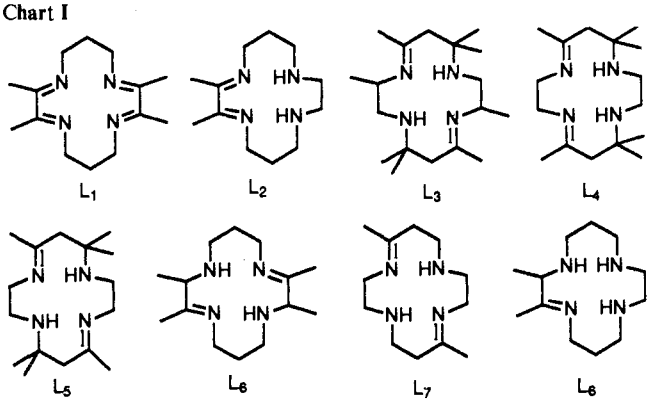

L_1 L_2 L_3 L_4 L_5 L_6 L_7 L_8

Experimental Section

Materials. The complexes $[CoL_1Br_2]Br$[14,15] (L_1 = 2,3,9,10-tetramethyl-1,4,8,11-tetraazacyclotetradeca-1,3,8,10-tetraene), $[CoL_2Br_2]ClO_4$[14,15] (L_2 = 2,3-dimethyl-1,4,8,11-tetraazacyclotetradeca-1,3-diene), $[CoL_3(H_2O)_n](ClO_4)_2$[16,17] (L_3 = 3,5,7,7,10,12,14,14-octamethyl-1,4,8,11-tetraazacyclotetradeca-4,11-diene, n = 1 or 2), $[CoL_4(H_2O)_n](ClO_4)_2$[18] (n = 1 or 2, L_4 = 5,7,7,12,12,14-hexamethyl-1,4,8,11-tetraazacyclotetradeca-4,14-diene), *N-rac*-$[CoL_5(H_2O)](ClO_4)_2$,[19,20] *N-meso*-$[CoL_5(H_2O)_2](ClO_4)_2$,[16,20] $[CoL_6Br_2]ClO_4$[21] (L_6 = 2,3,9,10-tetramethyl-1,4,8,11-tetraazacyclotetradeca-1,8-diene), $[CoL_7Br_2]ClO_4$[22] (L_7 = 5,12-dimethyl-1,4,8,11-tetraazacyclotetradeca-4,11-diene), and $[CoL_8Br_2]ClO_4$[21] (L_8 = 2,3-dimethyl-1,4,8,11-tetraazacyclotetradeca-1-ene) were prepared as previously described and characterized by UV–vis, IR, and ^1H NMR spectroscopies. (**Warning**: The perchlorate salts used in this study may be explosive and potential hazardous.) Analyses for cobalt and anions of these complexes were satisfactory.

Acetonitrile was purified in the published manner[23] and stored under vacuum over activated molecular sieves (3A) or CaH_2. Research grade CO_2 and CO were used.

Spectroscopic Measurements. For UV–vis measurements of the various cobalt(I) complexes, all of which require rigorous exclusion of oxygen and water, the (1–5) × 10^{-4} M solutions of the reduced species were made by bulk-electrolysis in a sealed cell[24] equipped with a reagent reservoir. Typically, 20 mL of a solution containing purified and degassed CH_3CN and electrolyte (0.1 M tetrapropylammonium perchlorate, TPAP) was stored in the reagent reservoir over activated alumina overnight under vacuum (or under <1 atm of CO_2 or CO). Then the solution was filtered into the cell through a frit and mixed with a weighed sample of the solid Co(II) or Co(III) complex. The entire cell assembly fitted into the cell compartment of a Cary 17 or 210 spectrophotometer. A magnetic stirrer pumped the solution over the working electrode and through a 10-mm optical cell. The bulk electrolyses were performed with a Princeton Applied Research Model 173 potentiostat with a Model 179 digital coulometer. The end point of the reduction (reached after 0.6 to 1.5 h) was determined by monitoring the coulometry

(4) Studies of structures of CO_2-containing complexes and reactions of metal complexes with CO_2: (a) Darensbourg, D. J.; Darensbourg, M. Y.; Goh, L. Y.; Ludvig, M.; Wiegreffe, P. *J. Am. Chem. Soc.* **1987**, *109*, 7539. (b) Baba, A.; Kashiwagi, H.; Matsuda, H. *Organometallics* **1987**, *6*, 137. (c) Walther, D.; Herzog, V. *Z. Chem.* **1987**, *27*, 373. (d) Braunstein, P.; Matt, D.; Nobel, D. *J. Am. Chem. Soc.* **1988**, *110*, 3207. (e) Mascetti, J.; Tranquille, M. *J. Phys. Chem.* **1988**, *92*, 2177. (f) Arafa, I. M.; Shin, K.; Goff, H. M. *J. Am. Chem. Soc.* **1988**, *110*, 5228. (g) Kaska, W. C.; Nemeh, S.; Shirazi, A.; Potuznik, S. *Organometallics* **1988**, *7*, 13. (h) Fochi, G. *J. Organomet. Chem.* **1988**, *350*, C1. (i) Buhro, W. E.; Chisholm, M. H.; Martin, J. D.; Huffman, J. C.; Folting, K.; Streib, W. E. *J. Am. Chem. Soc.* **1989**, *111*, 8149. (j) Pilato, R. S.; Geoffroy, G. L.; Rheingold, A. L. *J. Chem. Soc., Chem. Commun.* **1989**, 1287. (k) Walther, D. *Z. Chem.* **1989**, *29*, 146. (l) Reinking, M. K.; Ni, J.; Fanwick, P. E.; Kubiak, C. P. *J. Am. Chem. Soc.* **1989**, *111*, 6459. (m) Yasuda, H.; Okamoto, T.; Matsuoka, Y.; Nakamura, A.; Kai, Y.; Kanehisa, N.; Kasai, N. *Organometallics* **1989**, *8*, 1139. (n) Ruiz, J.; Guerchais, V.; Artruc, D. *J. Chem. Soc., Chem. Commun.* **1989**, 812. (o) Belforte, A.; Calderazzo, F. *J. Chem. Soc., Dalton Trans.* **1989**, 1007.

(5) Recent studies of photochemical or photoelectrochemical reduction of CO_2: (a) Ogura, K.; Arima, H. *Chem. Lett.* **1988**, 311. (b) Cook, R. L.; MacDuff, R. C.; Sammells, A. *J. Electrochem. Soc.* **1988**, *135*, 3070. (c) Belmore, K. A.; Vanderpool, R. A.; Tsai, J.-C.; Khan, M. A.; Nicholas, K. M. *J. Am. Chem. Soc.* **1988**, *110*, 2004. (d) Lemke, F. R.; DeLaet, D. L.; Gao, J.; Kubiak, C. P. *J. Am. Chem. Soc.* **1988**, *110*, 6904. (e) Willner, I.; Mandler, D. *J. Am. Chem. Soc.* **1989**, *111*, 1330. (f) Ikeda, S.; Saito, Y.; Yoshida, M.; Noda, H.; Maeda, M.; Ito, K. *J. Electroanal. Chem.* **1989**, *260*, 335. (g) Raphael, M. W.; Malati, M. A. *J. Photochem. Photobiol., A* **1989**, *46*, 367. (h) Bockris, J. O'M.; Wass, J. C. *J. Electrochem. Soc.* **1989**, *136*, 2521.

(6) Theoretical calculations for metal–CO_2 complexes: (a) Sasaki, S.; Kitaura, K.; Morokuma, K. *Inorg. Chem.* **1982**, *21*, 760. (b) Sasaki, S.; Kitaura, K.; Morokuma, K.; Ohkubo, K. *Inorg. Chem.* **1983**, *22*, 104. (c) Mealli, C.; Hoffmann, R.; Stockis, A. *Inorg. Chem.* **1984**, *23*, 56. (d) Sasaki, S.; Dedieu, A. *J. Organomet. Chem.* **1986**, *314*, C63. (e) Sasaki, S.; Dedieu, A. *Inorg. Chem.* **1987**, *26*, 3278. (f) Marcos, E. S.; Caballol, R.; Trinquier, G.; Barthelat, J.-C. *J. Chem. Soc., Dalton Trans.* **1987**, 2373. (g) Rosi, M.; Sgamellotti, A.; Tarantelli, F.; Floriani, C. *J. Organomet. Chem.* **1987**, *332*, 153. (h) Sasaki, S.; Ohkubo, K. *Inorg. Chem.* **1989**, *28*, 2583. (i) Sasaki, S.; Aizawa, N.; Koga, N.; Morokuma, K.; Ohkubo, K. *Inorg. Chem.* **1989**, *28*, 103. (j) Jeung, H. *Mol. Phys.* **1989**, *67*, 747.

(7) (a) Curtis, N. F. *J. Chem. Soc.* **1960**, 4409. Curtis, N. F.; Curtis, Y.; Powell, H. K. J. *J. Chem. Soc. A* **1966**, 1015. (b) Curtis, N. F. *Coord. Chem. Rev.* **1968**, *3*, 3.

(8) Brown, G. M.; Brunschwig, B. S.; Creutz, C.; Endicott, J. F.; Sutin, N. *J. Am. Chem. Soc.* **1979**, *101*, 1298.

(9) Fisher, B.; Eisenberg, R. *J. Am. Chem. Soc.* **1980**, *102*, 7361.

(10) Fujita, E.; Szalda, D. J.; Creutz, C.; Sutin, N. *J. Am. Chem. Soc.* **1988**, *110*, 4870.

(11) Gangi, D. A.; Durand, R. R. *J. Chem. Soc., Chem. Commun.* **1986**, 697.

(12) (a) Creutz, C.; Schwarz, H. A.; Wishart, J. F.; Fujita, E.; Sutin, N. *J. Am. Chem. Soc.* **1989**, *111*, 1153. (b) Creutz, C.; Schwarz, H. A.; Wishart, J. F.; Fujita, E.; Sutin, N. *J. Am. Chem. Soc.* Submitted for publication. (c) Szalda, D. J.; Fujita, E.; Creutz, C. *Inorg. Chem.* **1989**, *28*, 1446.

(13) Schmidt, M. H.; Miskelly, G. M.; Lewis, N. S. *J. Am. Chem. Soc.* **1990**, *112*, 3420–3426.

(14) Douglas, B. E., Editor-in-Chief *Inorganic Syntheses*; Wiley: New York, 1978; Vol. XVIII.

(15) Jackels, S. C.; Farmery, K.; Barefield, E. K.; Rose, N. J.; Busch, D. H. *Inorg. Chem.* **1972**, *11*, 2893.

(16) Rillema, D. P.; Endicott, J. F.; Papaconstantinou, E. *Inorg. Chem.* **1971**, *10*, 1739.

(17) Tait, A. M.; Busch, D. H. *Inorg. Nucl. Chem. Lett.* **1972**, *8*, 491.

(18) Love, J. L.; Powell, H. J. K. *Inorg. Nucl. Chem. Lett.* **1967**, *2*, 113.

(19) Goedken, V. L.; Kildahl, N. K.; Busch, D. H. *J. Coord. Chem.* **1977**, *7*, 89.

(20) Szalda, D. J.; Schwarz, C. L.; Endicott, J. F.; Fujita, E.; Creutz, C. *Inorg. Chem.* **1989**, *28*, 3214.

(21) Tait, A. M.; Busch, D. H. *Inorg. Chem.* **1977**, *16*, 966.

(22) Hay, R. W.; Lawrence, G. A. *J. Chem. Soc., Dalton Trans.* **1975**, 1466.

(23) Riddick, J. A.; Bunger, W. B.; Sakano, T. K. *Organic Solvents, Physical Properties and Methods of Purification*, 4th ed.; Wiley: New York, 1986.

(24) See diagram shown on p 494 in: Fajer, J.; Fujita, I.; Davis, M. S.; Forman, A.; Smith, K. M. In *Electrochemical and Spectrochemical Studies of Biological Redox Components*; Adv. Chem. Ser. 201; Kadish, K., Ed.; American Chemical Society: Washington, D.C., 1982.

Table I. Experimental Details of the X-ray Diffraction Study of $[Co^{I}L_3](ClO_4)$

mol formula	$[Co(N_4C_{18}H_{36})](ClO_4)$
a, Å	8.433 (2)
b, Å	18.333 (4)
c, Å	7.257 (2)
α, deg	100.22 (2)
β, deg	91.29 (2)
γ, deg	87.68 (2)
V, Å^3	1103 (1)
Z	2
mol wt	466.89
space group	$P\bar{1}$
ρ(calc), g cm^{-3}	1.406
radiation	Mo Kα (graphite monochromatized)
μ, cm^{-1}	9.66
transmission coeff	
max	0.8961
min	0.8583
R	0.085
R_w	0.105
reflcns collected	4251
reflcns used, $F_o > 3\sigma(F_o)$	1557
no. of variables	293
max shift/error, final cycle	less 0.2 (except for disordered perchlorate, 0.9)
temp, K	295

Table II. Selected Bond Distances and Angles in $[Co^{I}L_3](ClO_4)$

	molecule 1	molecule 2
	Distances, Å	
Co-N1	1.961 (11)	1.952 (12)
Co-N4	1.925 (12)	1.897 (13)
	Angles, deg	
N1-Co-N4	85.8 (5)	85.7 (5)

and the loss of isosbestic points. The reversibility of the reaction was always checked by regeneration of the parent compound by reversing the polarity of the working electrode and always gave a >90% yield of the parent.

For IR measurements of the $Co^{I}L-CO^{+}$ complexes (except for L = L_3, L_4, and L_5), ca. 7 mM CH_3CN solutions were made by bulk electrolysis under CO and transferred by syringe to a CO-flushed, vacuum-tight IR cell (0.5-mm path length). The spectra were immediately determined on a Nicolet MX-1 spectrometer or a Mattson Polaris FT-IR spectrometer. For L = L_3, L_4, and L_5, IR samples of $Co^{I}L-CO^{+}$ were prepared by the introduction of CO into solutions of the cobalt(I) complexes that had been prepared by sodium amalgam (Na-Hg) reduction[12c] in CH_3CN.

^1H NMR spectra were obtained on a Bruker AM-300 spectrometer. NMR samples of $Co^{I}L^{+}$ solutions in purified CD_3CN were prepared from $Co^{II}L^{2+}$ by Na-Hg reduction in sealed glassware.

Binding Constant Measurements. CO_2 and CO binding constants were determined by spectroscopic and/or electrochemical methods. For the spectroscopic determinations, a (0.1-2.5) × 10^{-3} M solution of $Co^{I}L^{+}$ in CH_3CN was prepared and frozen to liquid nitrogen temperature. Carbon dioxide (at known pressure and volume) was vacuum transferred to the cell containing a $Co^{I}L^{+}$ such that the final pressure of CO_2 was 0.05-1.6 atm. The concentration of CO_2 in the solution was calculated from the gas volume, the solution volume, and the partition coefficient. (At 25 °C, the ratio of the CO_2 concentration in CH_3CN to that in the gas phase is 6.84.) From the $Co^{I}L^{+}$, $Co^{I}L-CO_2^{+}$, and CO_2 concentrations, the binding constant was calculated. Since $CoL_3-CO_2^{+}$ and $CoL_4-CO_2^{+}$ decay rather rapidly to CO and cobalt(II) (half-lives, 8-30 min depending on the experimental conditions), the concentrations of $Co^{I}L^{+}$ were extrapolated to zero time from the kinetic data. Because of the small CO_2 binding constants and the intense colors of these $Co^{I}L^{+}$ complexes, the spectral changes resulting from the addition of CO_2 were dominated by the bleaching of the $Co^{I}L^{+}$ spectrum.

For CO binding-constant determinations, solutions (0.1-2.0) × 10^{-3} M in $Co^{I}L-CO^{+}$ were prepared from $Co^{I}L^{+}$ and CO, and then CO and solvent were evacuated from the cell.[12c] When fresh solvent was distilled into the cell, CO dissociation occurred to a small extent. From the $Co^{I}L^{+}$ and $Co^{I}L-CO^{+}$ absorbances and with the assumption of CO equilibration with gas and solution phases, the K_{CO} was obtained.

For the electrochemical determination of CO_2 binding constants, cyclic voltammetry was used.[11,13,25] Cyclic voltammograms were obtained on a BAS100 instrument with scan rates ranging from 2 mV s^{-1} to 10 V s^{-1}. The solutions used contained 1 mM cobalt complex and 0.1 M tetrapropylammonium perchlorate in CH_3CN. A conventional H-type cell was used, and the gas composition was 0, 3, 5, 10, 30, or 100% CO_2 in N_2 or Ar and 20, 50, or 100% CO in Ar. Glassy carbon, Pt, and SCE were used as working, counter and reference electrode, respectively. Ferrocene was also used as an internal standard.

The solubility of CO_2 in CH_3CN as a function of temperature was determined by adding a thermostated, CO_2-saturated CH_3CN sample to a known excess of aqueous $Ba(OH)_2$ which was back-titrated with standardized HCl. The solubility of CO in CH_3CN was measured by analyzing a CO-saturated CH_3CN solution on a Varian Model 3700 gas chromatograph equipped with a thermal conductivity detector and a molecular sieve 5A column at 60 °C (He carrier gas).

Collection and Reduction of X-ray Data. $[Co(N_4C_{18}H_{36})](ClO_4)$, $CoL_3(ClO_4)$, crystallized as dark blue prisms from a mixture of CH_3CN and THF at room temperature. The air-sensitive crystals were coated with petroleum jelly and mounted in a glass capillary. A crystal 0.12 × 0.16 × 0.47 mm^3 was used for data collection. An X-ray study of the crystals indicated triclinic space groups $P1$ (No. 1)[26a] or $P\bar{1}$ (No. 2).[26a] Crystal data and complete details of data collection and reduction are given in Table I and Table S1 (supplementary material).

Determination and Refinement of Structure. The Patterson map[27] and E-statistics indicated the correct space group as $P\bar{1}$ with the presence of two independent cobalt atoms in the asymmetric unit each situated on a crystallographic inversion center. A series of difference Fourier maps[27] were used to locate the remaining atoms in the asymmetric unit. The perchlorate anion was located in a general position with its oxygen atom disordered over two sets of positions each with a 50% occupancy factor. All non-hydrogen atoms were refined with use of anisotropic temperature parameters. Hydrogen atoms were placed at calculated positions (X-H = 0.95 Å) and allowed to "ride"[27] on the atom to which they were attached. A common isotropic temperature parameter for all the hydrogen atoms (U = 0.077 (9)) was included in the refinement. The quantity $\sum w(|F_o| - |F_c|)^2$ was minimized during the least-squares refinements with use of neutral atom scattering factors[26b] and anomalous dispersion effects.[26c]

Selected interatomic distances and angles are listed in Table II. Table S2 is a listing of observed and calculated structure factors, and the final thermal parameters for the non-hydrogen atoms are provided in Table S3. The calculated hydrogen atom positions are listed in Table S4. A complete listing of all interatomic bond distances and angles is given in Table S5. Final non-hydrogen atomic positional parameters are given in Table S7. (Tables S1-S7 are given in the supplementary material.)

Results

Description of the Structure. The two cobalt atoms in the asymmetric unit are situated on crystallographic inversion centers so that the two halves of the macrocycle are related by this inversion center. A view of one of the $Co^{I}L_3^{+}$ cations is shown in Figure 1. The macrocycle is in the N-meso form, with one amine hydrogen on either side of the plane defined by the cobalt and the four nitrogen atoms of the macrocycle. The cobalt(I) is square planar, being coordinated to the four nitrogen atoms of the macrocycle with an average Co-N (amine) bond length of 1.956 (12) Å and an average Co-N (imine) bond length of 1.911 (12) Å. These distances are similar to those observed in the five-coordinate complex[20] (*N-rac*-$Co^{II}L_5(OClO_3)^{+}$ and in the six-coordinate complex[12c] *N-meso*-$Co^{II}L_5Cl_2$. As can be seen in Figure 1, the methyl group on C(13) and one of the methyl groups on C(17) (in Figure 1, labeled C(13′) and C(17″)) are in axial positions on the same side of the plane of the macrocycle, while the inversion-related methyl groups are in axial positions on opposite sides of the macrocycle. The cobalt to C(13′) and to C(17″)

(25) (a) Bard, A. J.; Faulkner, L. R. *Electrochemical Methods, Fundamentals and Application*; John Wiley & Sons, Inc.: New York, 1980; p 34. (b) Gagné, R. R.; Allison, J. L.; Ingle, D. M. *Inorg. Chem.* **1979**, *18*, 2767.

(26) (a) *International Tables for X-ray Crystallography*, 3rd ed.; Kynoch Press: Birmingham, England, 1969; Vol. I, pp 74-75. (b) *Ibid.*; Vol. IV, pp 99-101 and 149-150. (c) Cromer, D. T.; Liberman, D. *J. Chem. Phys.* **1970**, *53*, 1891.

(27) Shelx-76: Sheldrick, G. M. In *Computing in Crystallography*; Shenk, H., Olthof-Hazekamp, R., van Koningsveld, H., Bassi, G. C., Delft University: Delft, Holland, 1978; pp 34-42.

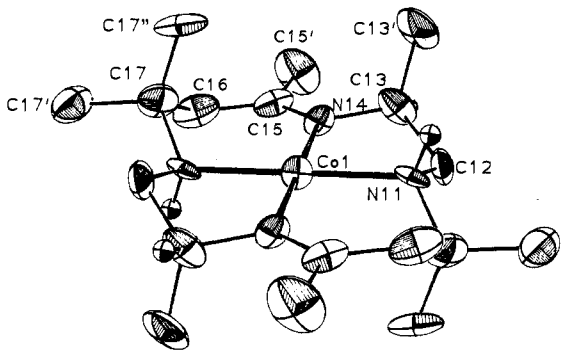

Figure 1. An ORTEP view of a $Co^{I}L_3^{+}$ cation. The thermal ellipsoids are at the 50% probability level and the methyl and methylene hydrogen atoms are omitted for clarity. The cobalt atom lies on a crystallographic inversion center, and the unlabeled atoms in the macrocycle are related to the labeled atoms by this inversion operation.

distances are 3.56 and 3.30 Å, respectively, and the C(13′)–C(17″) distance is 4.25 Å; these distances are similar to those observed on the blocked side in the five-coordinate complexes[10,12c,20] *N-rac*-$Co^{II}L_5(H_2O)^{2+}$, *N-rac*-$Co^{II}L_5(OClO_3)^{+}$, and *N-rac*-$(Co^{I}L_5)_2(\mu\text{-}CO_2H)^{3+}$. In this way the fifth and sixth coordination sites of the cobalt are essentially blocked by the axial methyl group of the macrocycle. The amine hydrogen atoms of the macrocycle are hydrogen bonded to oxygen atoms of the perchlorate ion (Table S6).

Solubility of Gases. The solubility of CO_2 in CH_3CN at 1 atm of CO_2 was determined to be 0.28 M at 25 °C, 0.24 M at 30 °C, 0.20 M at 40 °C, 0.14 M at 50 °C, 0.058 M at 70 °C, 0.044 M at 75 °C, and 0.026 M at 80 °C ($\Delta H° = -8.4 \pm 1.0$ kcal mol^{-1}, $\Delta S° = -30 \pm 4$ cal K^{-1} mol^{-1}). Dalton's law of partial pressure was found to hold within experimental error, and the solubility of CO_2 in a 0.1 M tetrapropylammonium perchlorate solution of CH_3CN was found to be the same as in pure CH_3CN. The solubility of CO in CH_3CN at 25 °C was found to be 0.0083 M at 1 atm of CO.

Preparation of Cobalt(I) Complexes. While sodium amalgam (0.5–1.0% Na in Hg) reduction is useful for the preparation of $Co^{I}L_3^{+}$ and $Co^{I}L_5^{+}$, bulk electrolysis proved the most useful general method for producing solutions of the cobalt(I) complexes. Reduction by Na–Hg has disadvantages for some of these complexes: $Co^{I}L_1^{+}$ and $Co^{I}L_2^{+}$ are further reduced by Na–Hg; the $Co^{I}L_6^{+}$, $Co^{I}L_7^{+}$, and $Co^{I}L_8^{+}$ complexes without an axial CO_2 or CO ligand undergo further reduction to cobalt(0) and/or degraded ligand; the reduction of any of the cobalt macrocycles with Na–Hg under CO produced $Co(CO)_4^{-}$, which has a carbonyl stretching band at 1892 cm^{-1} in CH_3CN (ascertained from an authentic sample of $Co(CO)_4^{-}$). Furthermore, Na–Hg reacts with CO_2.

Isomers. ^{1}H NMR spectra of cobalt(I) solutions generated from either *N-rac*-$CoL_5(ClO_4)_2$ or *N-meso*-$CoL_5(ClO_4)_2$ by Na–Hg reduction in CD_3CN were identical and consistent with the formation of an (85 ± 5)%:(15 ± 1)% equilibrium mixture of two isomers (determined by integration over all of the resonances of each component). Similarly, the ^{1}H NMR of a CD_3CN solution of $Co^{I}L_3^{+}$ suggests an (88 ± 5)%:(12 ± 1)% mixture of two isomers. Busch and co-workers have assigned the isomer resonances for the isoelectronic nickel(II) macrocycles in D_2O, acetone, and nitromethane;[28] we use the earlier assignments to assign our Ni(II) spectra determined in CD_3CN vs external TMS. These may be compared with those obtained for the cobalt complexes (both major and minor components of the mixtures): *N-meso*-$Ni^{II}L_5^{2+}$ 1.379 (eq CH_3), 1.634 (ax CH_3), and 2.106 (imine CH_3) ppm; *N-rac*-$Ni^{II}L_5^{2+}$ 1.188 (eq CH_3), 1.957 (ax CH_3), and 2.055 (imine CH_3) ppm; major $Co^{I}L_5^{+}$ 1.020, 1.467, and 1.853 ppm; minor $Co^{I}L_5^{+}$ 0.986, 1.689, and 1.750 ppm; major $Co^{I}L_3^{+}$ 0.969, 1.501, 1.858, and 1.214 (doublet, CH_3 of the five-membered ring) ppm; minor $Co^{I}L_3^{+}$ 1.732, 1.792 ppm (remaining resonances overlapped with other peaks). On the basis of this NMR work alone we would be inclined to assign the major component in both $Co^{I}L_5^{+}$ and $Co^{I}L_3^{+}$ solutions to the N-meso cobalt(I) isomer; for these the methyl resonances are almost equally spaced, as is seen for the N-meso nickel(II) complexes. However, as will be described, the behavior of cobalt(II) solutions and the electrochemical results for the CoL_5 isomers strongly suggest that *N-rac*-$Co^{I}L_5^{+}$ is the favored isomer. Thus we do not attempt to assign the resonances for the cobalt(I) complexes.

Over the 2–3-h period during which *N-meso*-$Co^{II}L_5^{2+}$ was reduced to Co^{I} in bulk electrolyses on a Pt electrode (either under vacuum or CO_2) and then reoxidized at the electrode, the 322-nm peak[20] of *N-meso*-$Co^{II}L_5^{2+}$ shifted to 310 nm, consistent with essentially complete (>90%) conversion to *N-rac*-$Co^{II}L_5^{2+}$. The ^{1}H NMR spectra of the two isomers (obtained by dissolving authentic[20] samples) of the paramagnetic complex differ significantly: N-meso, 3.02 and 4.17 ppm; N-rac, 5.71 and 7.48 ppm relative to external TMS in CD_3CN. From the integrated intensities of these peaks in a $Co^{II}L_5^{2+}$ solution produced in the decomposition of the CO_2 complex, the final mixture was 9% N-meso and 91% N-rac.

Because of the isomer equilibration on the electrolysis time scale we did not isolate the isomers of other cobalt macrocycles for

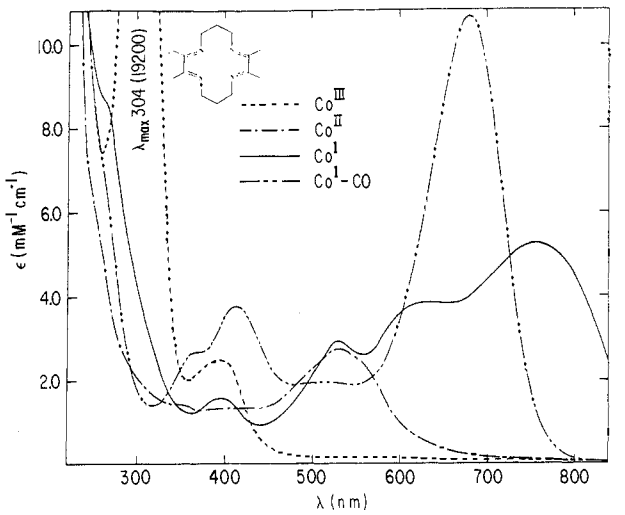

Figure 2. Absorption spectra of $Co^{III}L_3Br_2^{+}$, $Co^{II}L_1^{2+}$, $Co^{I}L_1^{+}$, and $Co^{I}L_1$–CO^{+} prepared by bulk electrolysis in a 0.1 M solution of TPAP in CH_3CN.

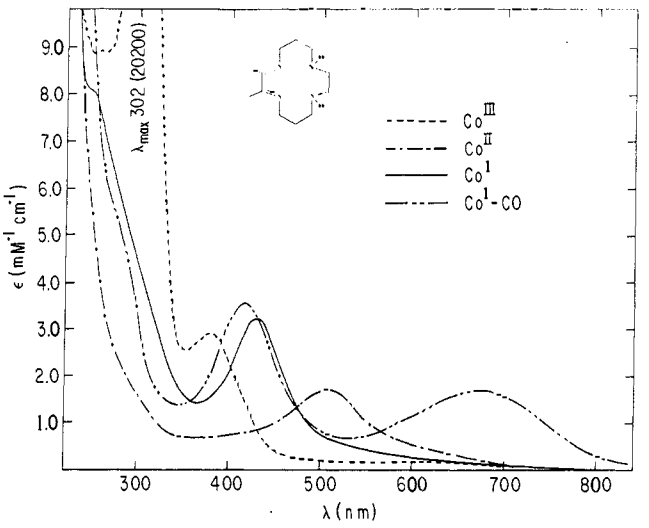

Figure 3. Absorption spectra of $Co^{III}L_2Br_2^{+}$, $Co^{II}L_2^{2+}$, $Co^{I}L_2^{+}$, and $Co^{I}L_2$–CO^{+} prepared by bulk electrolysis in a 0.1 M solution of TPAP in CH_3CN.

(28) Warner, L. G.; Rose, N. J.; Busch, D. H. *J. Am. Chem. Soc.* **1968**, *90*, 6938.

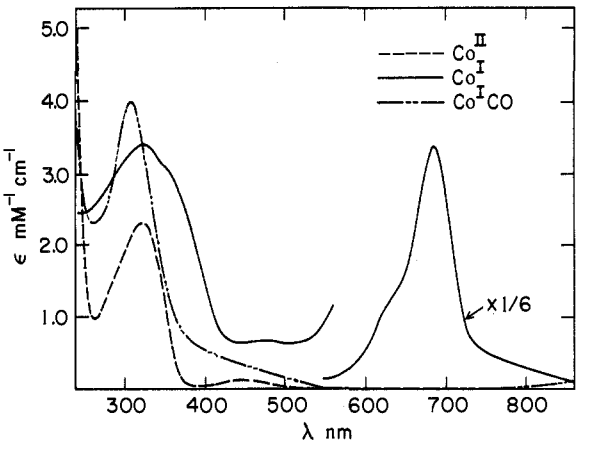

Figure 4. Absorption spectra of $Co^{II}L_3^{2+}$, $Co^{I}L_3^{+}$, and $Co^{I}L_3CO^{+}$ prepared by bulk electrolysis in a 0.1 M solution of TPAP in CH_3CN.

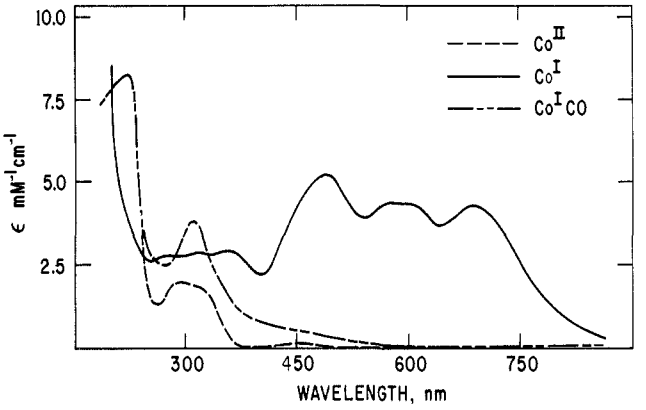

Figure 5. Absorption spectra of $Co^{II}L_4^{2+}$, $Co^{I}L_4^{+}$, and $Co^{I}L_4CO^{+}$ prepared by bulk electrolysis in a 0.1 M solution of TPAP in CH_3CN.

Table III. Electronic Absorption Spectra of Cobalt(III) and Cobalt(II) Macrocycles in CH_3CN[a]

complex	λ_{max}, nm (ϵ, M^{-1} cm^{-1})
	Cobalt(III) Complexes
$[CoL_1Br_2]Br$	598 (66), 394 (2460), 304 (19200)
$[CoL_2Br_2]ClO_4$	630 (116), 380 (2660), 302 (20200)
$[CoL_6Br_2]ClO_4$	650 (65), 370 sh (3730), 312 (15100), 260 sh (10300), 210 (17900)
$[CoL_7Cl_2]ClO_4$	616 (42), 440 sh (44), 320 sh (1380), 270 (18200), 228 (16700)
$[CoL_8Br_2]ClO_4$	662 (57), 376 (2900), 302 (18300), 217 (14200)
	Cobalt(II) Complexes
CoL_1^{2+}	570 sh (1680), 526 (2620), 470 sh (2070), 350 sh (1440), 250 sh (5930)
CoL_2^{2+}	510 (1650)
CoL_3^{2+}	1430 (43), 450 (129), 322 (2320), 210 (15300)
CoL_4^{2+}	1500 (41), 449 (157), 320 sh (1850), 297 (2050), 227 (8350)
CoL_5^{2+}[b]	1390 (42), 440 (120), 310 (2470), 209 (15500)
CoL_6^{2+}	440 sh (130), 320 sh (1910)
CoL_7^{2+}	440 sh (100), 338 (2070)
CoL_8^{2+}	460 sh (80), 330 (1030)

[a] The CH_3CN contains 0.1 M tetrapropylammonium perchlorate. [b] Reference 20.

studies of the CO_2 and CO binding constants by spectroscopic methods.

Characterization of Cobalt(I) Complexes. The electronic absorption spectra of the cobalt(I) complexes determined here are shown in Figures 2–5, together with the spectra of CO_2 and CO adducts. Table III summarizes the spectroscopic observations for the cobalt(II) and cobalt(III) complexes.

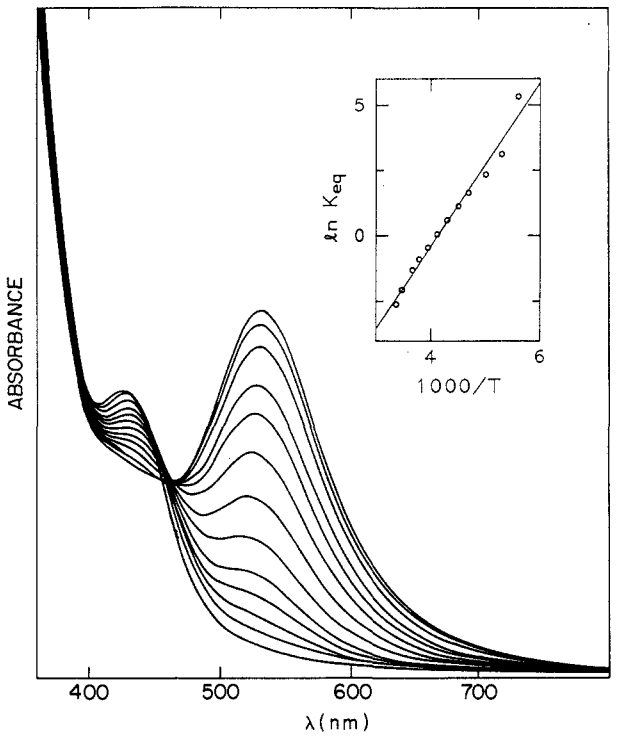

Figure 6. Temperature-dependent spectrum of *N-rac*-$Co^{I}L_5$–CO_2^{+} in C_3H_7CN. The peak at 530 nm diminishes upon cooling. The spectra were taken at 40.0, 23.8, 14.8, 0.0, −9.0, −20.0, −30.5, −40.8, −51.5, −60.2, −73.6, −84.5, and −110.5 °C. Insert: Relationship between $1000/T$ and ln (K_{eq}) (eqs 1 and 2).

Carbon Dioxide Binding. Although the $Co^{II/I}$ cyclic voltammograms of the CoL_1 and CoL_2 complexes were the same under Ar and CO_2, we carried out bulk electrolyses of the complexes under CO_2 to determine whether these might react slowly with CO_2. The UV–vis spectra of the cobalt(I) species are identical under vacuum and CO_2. Thus these Co(I) complexes seem to be unreactive toward CO_2.

The $Co^{I}L_3(CO_2)^{+}$, $Co^{I}L_4(CO_2)^{+}$, and *N-rac*-$Co^{I}L_5(CO_2)^{+}$ complexes were readily prepared by Na–Hg reduction followed by introduction of CO_2. This approach was used earlier[10] to characterize the equilibrium between *N-rac*-$Co^{I}L_5^{+}$ and *N-rac*-$Co^{I}L_5(CO_2)^{+}$ as a function of temperature ($\Delta H° = -5.4 \pm 1$ kcal mol^{-1}, $\Delta S° = +0.4 \pm 3$ cal K^{-1} mol^{-1}). From the earlier results and the temperature dependence of the solubility of CO_2 in CH_3CN given above, the parameters for formation of this CO_2 complex with gaseous CO_2 as standard state are $\Delta H° = -13.8 \pm 1$ kcal mol^{-1} and $\Delta S° = -30 \pm 3$ cal K^{-1} mol^{-1}. When a purple solution of *N-rac*-$CoL_5(CO_2)^{+}$ is cooled, the solution becomes brownish yellow and freezes as a yellow solid, but the purple color returns when the solution is warmed to room temperature. This thermochromism, which seems[10,12a] to be due to the addition of solvent molecule to 5-coordinated $Co^{I}L_5(CO_2)^{+}$ as shown in eq 1 and 2, was studied in both CH_3CN and C_3H_7CN, which has the advantage of a greater liquid range and of forming a glass at low temperature. The temperature dependence of the spectrum

$$Co^{I}L_5\text{–}CO_2^{+} + S \rightleftharpoons S\text{–}Co^{I}L_5\text{–}CO_2^{+}\ (S = CH_3CN, C_3H_7CN) \quad (1)$$

$$K_s = [S\text{–}Co^{I}L_5\text{–}CO_2^{+}]/[Co^{I}L_5\text{–}CO_2^{+}] \quad (2)$$

in C_3H_7CN is shown in Figure 6. The 530-nm band diminishes in intensity and a 430-nm shoulder increases in intensity as the temperature drops. Assuming that the 40 and −110 °C spectra represent complete conversion to the high- and low-temperature forms, respectively, K_s can be calculated from the intensity of the 530-nm band as a function of temperature. The temperature dependence of K_s determined in this way is shown in Figure 6. Measurements over the range −110 to 40 °C in C_3H_7CN yield

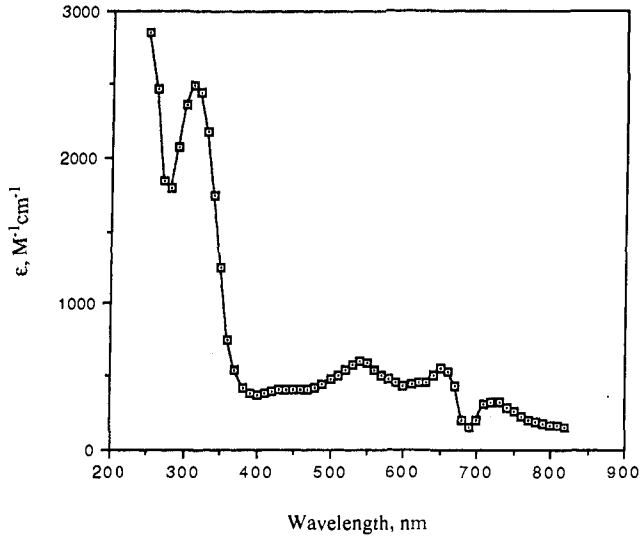

Figure 7. Calculated spectrum for $Co^{I}L_3$–CO_2^+ from a mixture of $Co^{I}L_3^+$ and its CO_2 adduct in CH_3CN. The peak and dip between 600 and 700 nm are an artifact due to the subtraction of the intense absorption.

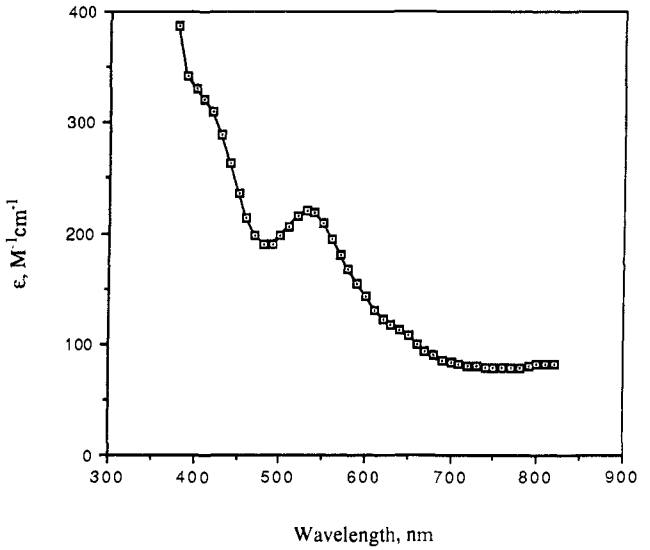

Figure 8. Calculated spectrum for $Co^{I}L_4$–CO_2^+ from a mixture of $Co^{I}L_4^+$ and its CO_2 adduct in CH_3CN.

$K_s(298) = 0.08 \pm 0.06$, $\Delta G°(298) = 1.5 \pm 0.4$ kcal mol^{-1}, $\Delta H° = -6.2 \pm 0.3$ kcal mol^{-1}, and $\Delta S° = -26 \pm 1$ cal K^{-1} mol^{-1}. Measurements over the range −40 to 40 °C in CH_3CN give $K_s(298) = 0.11 \pm 0.13$, $\Delta G°(298) = 1.3 \pm 0.7$ kcal mol^{-1}, $\Delta H° = -7.0 \pm 0.4$ kcal mol^{-1}, and $\Delta S° = -28 \pm 2$ cal K^{-1} mol^{-1}. A solid tan sample, obtained at −70 °C from a THF–CH_3CN mixture, shows $\nu_{C=N}$ 1653 cm^{-1}, $\nu_{C=O}$ 1558 cm^{-1}, and two kinds of $\nu_{C\equiv N}$, 2337 cm^{-1} for coordinated CH_3CN and 2272 cm^{-1} for free CH_3CN, consistent with the formation of [S–$Co^{I}L_5$–CO_2^+](ClO_4) with S = CH_3CN.

In the case of $Co^{I}L_3^+$ and $Co^{I}L_4^+$, due to the small CO_2 binding constants, the spectra at 25 °C under 1 atm of CO_2 consisted of a mixture of Co(I) (which contributes intense color) and the CO_2 adduct. The spectra of $Co^{I}L_3$–CO_2^+ and $Co^{I}L_4$–CO_2^+, which are shown in Figures 7 and 8, were obtained by correcting the observed spectra for the free (equilibrium concentration) cobalt(I). The CH_3CN solutions of CoL_3–CO_2^+ and CoL_4–CO_2^+ decay to produce CO and H_2. These reactions seem to be about 10 times faster than that[10] of CoL_5–CO_2^+ under comparable conditions. The results of the binding studies are presented in Table IV. The averaged binding constants are 4.0 ± 1.3 M^{-1} for $Co^{I}L_3^+$ and 26 ± 8 M^{-1} for $Co^{I}L_4^+$. We could not determine whether CoL_3–$(CO_2)^+$ and $CoL_4(CO_2)^+$ exhibit thermochromic behavior because of their low binding ability and high reactivity: When dark solutions containing a mixture of Co(I) and the CO_2 adduct under 1 atm of CO_2 were cooled, the solutions became lighter in color because of the production of more CO_2 adduct—a consequence of the higher solubility of CO_2 at low temperature. For *N-meso*-$Co^{I}L_5^+$, the absorption spectrum and binding constant could not be determined by spectroscopic methods because the Co(I) solution was an equilibrium (largely *N-rac*-$Co^{I}L_5^+$) mixture.

Although the $Co^{I}L_6^+$, $Co^{I}L_7^+$, and $Co^{I}L_8^+$ complexes could not be prepared in CH_3CN by bulk electrolysis in vacuo, their CO_2 complexes were readily prepared by bulk electrolysis under CO_2. Their spectra are shown in Figures 9–11 together with the spectra of the corresponding Co^{I}–CO adducts. These yellow CO_2 adducts no longer have a 530-nm band but exhibit only a 450–480-nm shoulder.

Table IV. Spectroscopic Determination of CO_2 Binding Constants for $Co^{I}L_3^+$ and $Co^{I}L_4^+$ at 25 °C

L	$[CO_2]$, M	original $[Co^{I}]$, mM	equil $[Co^{I}]$,[a] mM	K_{CO_2}, M^{-1}
L_3	0.017	0.648	0.609	3.8
L_3	0.055	0.797	0.679	3.2
L_3	0.100	0.097	0.057	6.9
L_3	0.116	0.485	0.382	3.8
L_3	0.191	0.166	0.093	4.1
L_3	0.281	0.599	0.226	5.9
L_3	0.315	0.564	0.285	3.4
L_3	0.444	0.110	0.050	3.5
L_3	0.463	0.682	0.293	3.1
L_4	0.015	0.557	0.382	31
L_4	0.017	2.50	1.62	32
L_4	0.083	0.471	0.115	37
L_4	0.098	2.50	0.746	24
L_4	0.141	0.557	0.158	18
L_4	0.148	2.50	0.711	17
L_4	0.443	0.471	0.044	22

[a] The concentrations were estimated by extrapolation to time = 0.

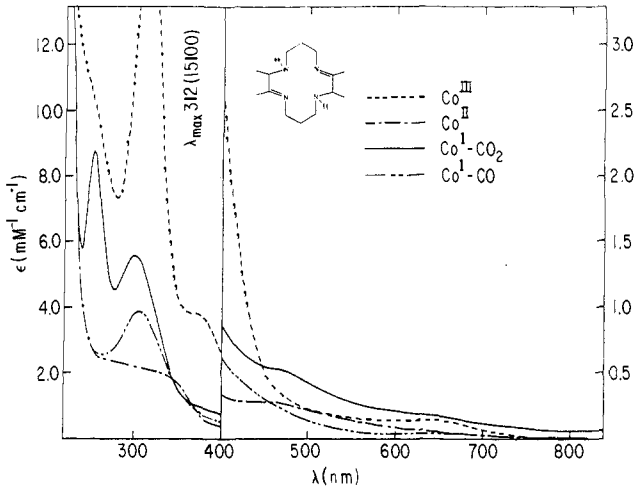

Figure 9. Absorption spectra of $Co^{III}L_6Br_2^+$, $Co^{II}L_6^{2+}$, $Co^{I}L_6$–CO_2^+, and $Co^{I}L_6CO^+$ prepared by bulk electrolysis in a 0.1 M solution of TPAP in CH_3CN.

Electrochemical Studies. Our results for the $Co^{II/I}$ potentials under argon are the same as those of Busch and co-workers[29] within experimental error, except for CoL_8. We obtained $E_{1/2} = -1.65$ V for $[CoL_8Br_2]ClO_4$, which exhibited irreversibility at scan rates below 1 V s^{-1}.

In the presence of CO_2, cyclic voltammograms of the cobalt macrocycles exhibited three kinds of behavior in CH_3CN at scan

(29) Tait, A. M.; Lovecchio, F. V.; Busch, D. H. *Inorg. Chem.* **1977**, *16*, 2206.

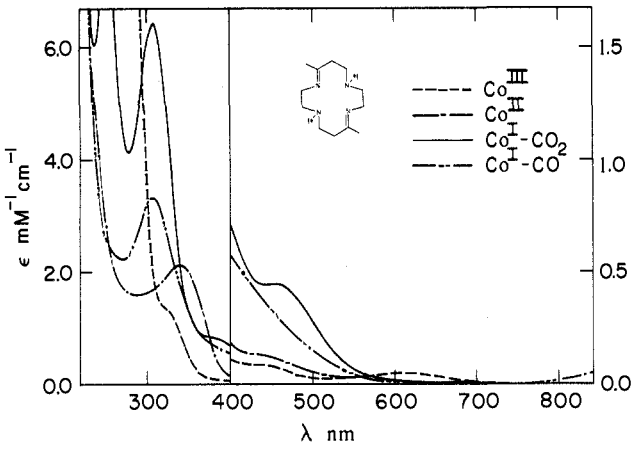

Figure 10. Absorption spectra of $Co^{III}L_7Cl_2^+$, $Co^{II}L_7^{2+}$, $Co^{I}L_7$–CO_2^+, and $Co^{I}L_7CO^+$ prepared by bulk electrolysis in a 0.1 M solution of TPAP in CH_3CN.

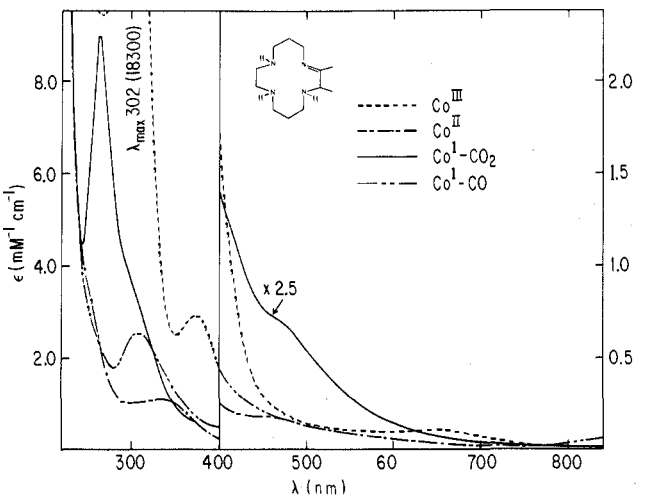

Figure 11. Absorption spectra of $Co^{III}L_8Br_2^+$, $Co^{II}L_8^{2+}$, $Co^{I}L_8$–CO_2^+, and $[Co^{I}L_8CO]^+$ prepared by bulk electrolysis in a 0.1 M solution of TPAP in CH_3CN.

Scheme I

$$Co^{II}L_i^{2+} + e^- \rightleftharpoons Co^{I}L_i^+ \quad (3)$$

$$Co^{I}L_i^+ + CO_2 \underset{k_b}{\overset{k_f[CO_2]}{\rightleftharpoons}} Co^{I}L_i\text{–}CO_2^+ \quad (4)$$

$$K_{CO_2} = [Co^{I}L_i\text{–}CO_2^+]/\{[Co^{I}L_i^+][CO_2]\} = k_f/k_b \quad (5)$$

rates of 100 and 200 mV s^{-1}. (a) No change was observed in the $Co^{II/I}$ voltammograms for $[CoL_1Br_2]Br$ and $[CoL_2Br_2]ClO_4$. (b) The voltammogram retained its reversible profile but shifted toward more positive potentials with increasing CO_2 concentration for the solutions of $CoL_3(ClO_4)_2$, $CoL_4(ClO_4)_2$, *N-meso*-$CoL_5(ClO_4)_2$, and $[CoL_6Br_2]ClO_4$. (The oxidation waves of CoL_6–CO_2^+ were ill-defined with larger current for the reduction and smaller current for the oxidation, and large differences of E_{pc} and E_{pa} were observed.) (c) Only the cathodic component of the voltammogram was observed for *N-rac*-$CoL_5(ClO_4)_2$, $[CoL_7Br_2]ClO_4$, and $[CoL_8Br_2]ClO_4$ under these conditions. When the scan rate was decreased to 2–10 mV s^{-1}, and the CO_2 concentration decreased to 0.003–0.08 M, ill-defined oxidation waves appeared for these complexes.

This range of behavior is consistent with the operation of an EC mechanism[25a,30] as shown in Scheme I. In case a, the binding constants K_{CO_2} (eq 5) are very small ($K_{CO_2} < 0.5$ M^{-1}) or the

(30) Nicholson, R. S.; Shain, I. *Anal. Chem.* **1964**, *36*, 706.

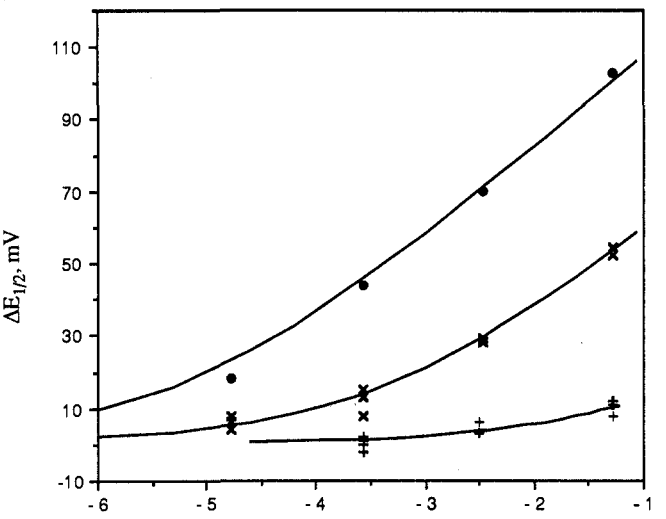

Figure 12. Relationship between ln $[CO_2]$ and $\Delta E_{1/2}$ for *N-meso*-$Co^{I}L_5^+$ (●: line calculated from eq 6 with $K = 165$ M^{-1}), $Co^{I}L_4^+$ (×: solid curve calculated from eq 6 with $K_{CO_2} = 25$ M^{-1}), and $Co^{I}L_3^+$ (+: solid curve calculated from eq 6 with $K_{CO_2} = 1.7$ M^{-1}).

forward rate constants k_f are very small, so that essentially no chemical reaction takes place during the experiment. L_1 and L_2 lie in this limit. Case b is an E_rC_r system, where electron transfer and forward and backward reactions are sufficiently rapid and K_{CO_2} is relatively large, so that the system is always in equilibrium as shown in eq 6. The effect of the chemical reaction can be seen

$$E = E^\circ + (RT/nF) \ln \{1 + [CO_2]K_{CO_2}\} \quad (6)$$

as a displacement of the reversible wave toward more positive potentials. In the case of $K_{CO_2} \gg 100$ M^{-1}, the binding constants are easily evaluated from the linear correlation of the observed shift in $E_{1/2}$ (the average of E_{pc} and E_{pa}) with ln $[CO_2]$ with a slope of 0.026 V ($n = 1$) per decade. For the case of $K_{CO_2} \leq 10^2$ M^{-1}, the observed shift in $E_{1/2}$ is not a linear function of ln $[CO_2]$. The values $K_{CO_2} = 165 \pm 15$ M^{-1} for *N-meso*-$Co^{I}L_5^+$, $K_{CO_2} = 25 \pm 6$ M^{-1} for $Co^{I}L_4^+$, and $K_{CO_2} = 1.7 \pm 0.5$ M^{-1} for $Co^{I}L_3^+$ were obtained by fitting the experimental data with eq 6 as shown in Figure 12. Case c is a limiting case of the E_rC_r system, where electron transfer and forward reactions are sufficiently rapid but the reverse reaction is slow (K_{CO_2} is also large). The CO_2 adduct oxidizes at a more positive potential (>0.0 V). (Since the height of the cathodic peak was almost the same as that under Ar and catalytic reduction of CO_2 is known to be slow[10] under these conditions, we eliminated the possibility of electron transfer followed by a catalytic reaction.) CO^{I}-L_6, -L_7, -L_8 and *N-rac*-L_5 lie in this limit. In order to elucidate the kinetics, thermodynamics, and solvent effects of CO_2 binding to Co macrocycles in various solvents, a simulation study of the cyclic voltammograms is currently in progress.[31] Our preliminary results indicate that the binding constants (M^{-1}) are the following: $(6 \pm 2) \times 10^4$ for *N-rac*-CoL_5^+, $(9 \pm 3) \times 10^4$ for CoL_6^+, $(7 \pm 3) \times 10^5$ for CoL_7^+, and $(3 \pm 2) \times 10^6$ for CoL_8^+ in CH_3CN.

The CO_2 binding constants determined for *N-rac*-$Co^{I}L_5^+$ by cyclic voltammetry ($(6 \pm 2) \times 10^4$ M^{-1}) and earlier[10] by electronic spectroscopy ($(1.2 \pm 0.5) \times 10^4$ M^{-1}) differ by a factor of 5. Because of the very different time scales for the two measurements and the operation of *N-rac*/*N-meso*-Co^{I} isomerism, the two methods should give slightly (<20%) different values (the spectroscopic method should give a value smaller by approximately a factor $\{K^{I}_{m,r}/(1 + K^{I}_{m,r})\}$), but not such different values as are

(31) For a wide range of organic solvents, the magnitude of the CO_2 binding constant for $Co(I)L_5$ is similar, but the rate of CO_2 addition does seem to vary with solvent. Fujita, E.; Brunschwig, B. S.; Creutz, C. Work in progress.

Scheme II

$$Co^{II}L_i^{2+} + e^- \rightleftharpoons Co^{I}L_i^{+} \quad (3)$$

$$Co^{I}L_i^{+} + CO \rightleftharpoons Co^{I}L_i\text{–}CO^{+} \quad K^{I}_{CO} \quad (7)$$

$$Co^{I}L_i\text{–}CO^{+} - e^- \rightleftharpoons Co^{II}L_i\text{–}CO^{2+} \quad (8)$$

$$Co^{II}L_i\text{–}CO^{2+} \rightleftharpoons Co^{II}L_i^{2+} + CO \quad K^{II}_{-CO} \quad (9)$$

observed. This disagreement likely results from the differing media used (no electrolyte was added in the earlier work) or signals that we have underestimated our errors.

CO Binding. Gagné and Ingle determined[32] $K_{CO} = 4.7 \times 10^4$ M^{-1} for $Ni^{I}L_5^{+}$ in DMF using an electrochemical technique described above as case b. For L_1 and L_2, this approach also proved tractable for the cobalt macrocycles in CH_3CN (although ($E_{pa} - E_{pc}$) was ca. 90 mV rather than the ideal 58 mV, even with scan rates <25 mV s^{-1}). This method yielded $K_{CO} = (3 \pm 2) \times 10^4$ and $K_{CO} = (1.1 \pm 0.6) \times 10^5$ M^{-1}, for L_1 and L_2, respectively, at 24 ± 1 °C in good agreement with the spectrophotometric results (see below). However, for L_3 to L_8, in the presence of carbon monoxide, the cobalt macrocycles gave well-separated, irreversible cathodic and anodic waves, consistent with the operation of a E_rC_i mechanism (a rapid reduction followed by a rapid CO binding, and a rapid oxidation of Co^{I}–CO^{+} followed by rapid removal of CO, Scheme II), with large K^{I}_{CO} in eq 7 and K^{II}_{-CO} in eq 9.

Electronic absorption spectra of new CO adducts are shown in Figures 1–5 and 9–11 and are summarized in Table V, along with $Co(I)L_i^{+}$ spectra. Table VI summarizes the UV–vis spectra of the CO_2 adducts. Values of K_{CO_2} and K_{CO} (which was determined by the extent of Co^{I}–CO dissociation upon the removal of CO from the Co^{I}–CO system with UV–vis spectroscopy as previously described[12c]) and $\nu_{C\equiv O}$ are summarized in Table VII. $Co^{I}L_8(CO)^{+}$ exhibits an intense C≡O stretching band at 1912 cm^{-1} in addition to a weak band at 1895 cm^{-1}. Since the intensity ratio of the bands remained the same throughout the process of $Co^{II}L_8^{2+}$ reduction under CO, these two bands probably arise from different isomers. It is thus unlikely that $Co(CO)_4^{-}$ ($\nu_{C\equiv O}$ = 1892 cm^{-1}), which is normally produced from further reduction of Co^{I}, is responsible for the band at 1895 cm^{-1} in this experiment.

Discussion

Isomerism. Macrocycle isomerism is an important issue for the complexes studied here. First, except for L_1, there is conformational isomerism, as mentioned earlier. In addition, for five- or six-coordinate complexes containing *N-rac*-L, there is also positional isomerism. This is illustrated below for $CoL_5(CO_2)(S)^{+}$ in which a solvent molecule S is bound trans to the CO_2. If the open face of the N-rac isomer is denoted "primary" and the face toward which the axial methyl groups point is denoted "secondary", the two isomers are termed primary CO_2, S and secondary CO_2, S.

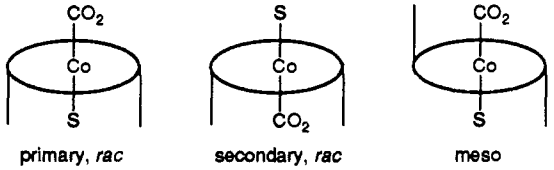

In the case of L_5, N-meso and N-rac isomers of the cobalt(II) complex have been identified and their rates of interconversion studied in water and organic solvents.[20] Equilibration of the *N-meso-* and *N-rac*-$Co^{II}L_5^{2+}$ isomers in CH_3CN is slow at room temperature. On the time scale of pulse radiolysis[12a,b] and cyclic voltammetry, the N-meso isomer retains its conformation upon reduction of $Co^{II}L_5^{2+}$ to cobalt(I) and exhibits different properties from the N-rac isomer. However, over the 2–3-h period required to reduce *N-meso*-$Co^{II}L_5^{2+}$ to Co^{I} in bulk electrolyses on a Pt electrode (either under vacuum or CO_2) and then reoxidize it at the electrode, the UV–vis spectrum[20] of the resulting solution indicated ≥90% conversion to *N-rac*-$Co^{II}L_5^{2+}$ and the ^1H NMR spectrum of the product solution from CO_2 reduction consisted of 91% N-rac and 9% N-meso isomers. These experiments indicate that, for $Co^{II}L_5^{2+}$, the N-rac form is the more stable at room temperature in acetonitrile (eq 10; $K^{II}_{m,r} = 91/9 \sim 10$). A similar conclusion has been drawn for $Co^{II}L_5^{2+}$ in water.[20] Within error

$$N\text{-}meso\text{-}Co^{II}L^{2+} \rightleftharpoons N\text{-}rac\text{-}Co^{II}L^{2+} \quad K^{II}_{m,r} \quad (10)$$

(±0.015 V), both $Co^{II}L_5^{2+}$ isomers are reduced at the same potential, $E_{1/2}$(N-rac) = $E_{1/2}$(N-meso). This observation requires that the equilibrium constants for eqs 10 and 11 be similar and that the dominant form of $Co^{I}L_5^{+}$ be N-rac. The ^1H NMR

$$N\text{-}meso\text{-}Co^{I}L^{+} \rightleftharpoons N\text{-}rac\text{-}Co^{I}L^{+} \quad K^{I}_{m,r} \quad (11)$$

studies of $Co^{I}L_5^{+}$ indicate an equilibrium isomer ratio of 85:15 ($K^{I}_{m,r} \sim 6$). On this basis the $E_{1/2}$ values for the two isomers should differ by 0.01–0.02 V, which lies within our experimental error. From the structures of *N-meso-* and *N-rac*-$Co^{II}L_5^{2+}$ isomers[12c,20] and that of *N-meso*-$Co^{I}L_3^{+}$, the origin of the preference of CoL_5 for the N-rac configuration is not obvious. However, for square-planar $Ni^{II}L_5^{2+}$ N-rac is also favored over N-meso.[28]

Since $Co^{II}L_5^{2+}$ isomerization is normally very slow, $Co^{I}L_5^{+}$

Table V. Electronic Absorption Spectra of Cobalt(I) Complexes in Acetonitrile at 25 °C[a]

	$E_{1/2}$, V vs SCE	λ_{max}, nm (ϵ, M^{-1} cm^{-1})
		CoL^{+}
L_1	−0.34	755 (5120), 630 sh (3690), 530 (2770), 392 (1490), 260 sh (8320)
L_2	−0.89	428 (3120), 250 sh (7770)
L_3	−1.28	685 (19500), 370 sh, 320 (3100)
L_4	−1.34	710 (4200), 600 sh (4280), 578 (4500), 485 (5420), 358 (3000), 320 (2950)
L_5	−1.34	678 (18000), 360 (3300), 308 (3500)[b]
L_7	−1.51	658, 360 sh
		$CoL(CO)^{+}$
L_1		675 (10600), 520 (1690), 414 (3300), 392 (1490), 370 sh (2350), 260 sh (5820)
L_2		675 (1670), 416 (3520), 270 sh (5750)
L_3		1030 (480), 495 sh (270), 310 (4000), 211 (11500)
L_4		1065 (250), 440 sh (670), 312 (3930), 223 (8470)
L_5		1040 (240), 510 (360), 430 sh, 310 (3900)
L_6		1030 (150), 670 (84),[c] 306 (3980)
L_7		1060 (220), 306 (3130), 215 sh (10800)
L_8		1020 (130), 306 (2470)

[a] The CH_3CN contains 0.1 M tetrapropylammonium perchlorate. Molar absorptivities of Co^{I} and Co^{I}–CO complexes assume 100% conversion from the parent Co(II) complexes. [b] Predominantly the N-rac isomer; see text. [c] This peak is probably due to a small amount of $Co^{I}L_1(CO)$.

Table VI. Electronic Absorption Spectra of $CoL(CO_2)^{+}$ Complexes in Acetonitrile at 25 °C[a]

	λ_{max}, nm (ϵ, M^{-1} cm^{-1})
L_3	535 (600), 460 sh (410), 310 (2490)[b]
L_4	540 (220), 400 sh (330), 310 (1750)[b]
L_5	530 (900), 430 sh, 310 (6040) 430 (ca. 700)[c]
L_6	470 sh (340), 440 sh (640), 300 (5440), 254 (8680)
L_7	450 sh (400), 380 sh (810), 306 (6400), 250 (7700)
L_8	480 sh (110), 390 sh (260), 300 sh (3700), 262 (9050)

[a] The CH_3CN contains 0.1 M tetrapropylammonium perchlorate. Molar absorptivities assume 100% conversion from the parent Co(II) complexes. [b] Due to the decomposition of the complex to Co(II) during the measurements, the ϵ may contain some error associated with the formation of the corresponding Co(II) complex. [c] In C_3H_7CN at −110.5 °C.

(32) (a) Gagné, R. R.; Ingle, D. M. *J. Am. Chem. Soc.* **1980**, *102*, 1444. (b) Gagné, R. R.; Ingle, D. M. *Inorg. Chem.* **1981**, *20*, 420.

Table VII. CO_2 and CO Binding Constants and Carbonyl Vibrational Frequencies for Cobalt Macrocycles in CH_3CN at 25 °C

macrocycle		$E_{1/2}$, V vs SCE	K_{CO_2}(elec), M^{-1}	K_{CO_2}(spec), M^{-1}	K_{CO}, M^{-1}	$\nu_{C\equiv O}$, cm^{-1}
Me_4[14]1,3,8,10-tetraene	L_1	−0.34	<0.5		5×10^4	2007
Me_2[14]1,3-diene	L_2	−0.89	<0.5		1.4×10^5	1959
Me_8[14]4,11-diene	L_3	−1.28	1.7 ± 0.5	4.0 ± 1.3	1.1×10^8	1912
Me_6[14]4,14-diene	L_4	−1.34	25 ± 6	26 ± 8	1.9×10^8	1918
N-meso-Me_6[14]4,11-diene	*N-meso*-L_5	−1.34	165 ± 15			
N-rac-Me_6[14]4,11-diene	*N-rac*-L_5	−1.34	$(6 \pm 2) \times 10^4$	$(1.2 \pm 0.5) \times 10^4$	2.3×10^8	1916
Me_4[14]1,8-diene	L_6	−1.41	$(9 \pm 3) \times 10^4$		$\geq 3 \times 10^8$	1910
Me_2[14]4,11-diene	L_7	−1.51	$(7 \pm 3) \times 10^5$		$\geq 3 \times 10^8$	1915
Me_2[14]1-ene	L_8	−1.65	$(3 \pm 2) \times 10^6$		$\geq 3 \times 10^8$	1912, 1895

isomerization is relatively rapid, and $Co^{II}L_5^{2+}$ isomerization is accelerated under the electrolysis conditions, it is likely that N-meso and N-rac forms of the cobalt(II) macrocycle equilibrate through an electron-transfer mechanism, i.e.

$$N\text{-}meso\text{-}Co^{II}L^{2+} \rightleftharpoons N\text{-}rac\text{-}Co^{II}L^{2+} \quad \text{slow} \qquad (10)$$

$$N\text{-}meso\text{-}Co^{I}L^{+} \rightleftharpoons N\text{-}rac\text{-}Co^{I}L^{+} \quad \text{"rapid"} \qquad (11)$$

$$N\text{-}meso\text{-}CoL^{2+} + N\text{-}rac\text{-}CoL^{+} \rightleftharpoons N\text{-}meso\text{-}CoL^{+} + N\text{-}rac\text{-}CoL^{2+} \qquad (12)$$

The outer-sphere electron-transfer reaction, eq 12, is expected to be rapid since only small nuclear configuration changes (metal–ligand and intraligand distances) accompany the reduction of the cobalt(II) complex to cobalt(I). (See the Results section.) The observation that eq 11 is so much faster than eq 10 is striking and could suggest a special mechanism for eq 11, perhaps involving inter- or intramolecular proton transfer from an N–H group to cobalt(I) (to give a hydride complex[12a]), followed by inversion about the nitrogen (resulting in macrocycle isomerization), followed by deprotonation of the metal center.[33]

Except for L_1, L_3, and L_8, there are two "conformational" isomers of $Co^{I}L_i^{+}$ and three "positional" isomers of CoL_i–CO^{+} or CoL_i–CO_2^{+}; for L_3, there are seven and thirteen isomers, respectively (the large number arises from the presence of both N- and C-chiral centers); for the monoene L_8, there are eight and sixteen isomers, respectively. With the exception of L_5, our work was done with samples whose isomer composition is not known. On the basis of our work with L_5,[12,20] we expect the nature of the isomer to have only negligible effects on the cobalt(II)/(I) reduction potential, on the absorption spectrum of $Co^{I}L^{+}$, and even on the magnitude[12] of the CO binding constant. However, as is discussed in detail later, the interaction of CO_2 with the macrocyclic complexes is sensitive to the nature of the macrocycle conformation.

Nature of the Cobalt(II) Reduction Products. The $Co(II)L^{2+}$ complexes used here are low-spin d^7 species. In the case of L_3 and L_5, reduction yields diamagnetic, low-spin d^8 cobalt(I) complexes (indicated by ^1H NMR studies). The similarity of the electronic absorption spectra for the reduced complexes of L_4 and L_7 to those of L_3 and L_5 indicates that these too are metal-reduction products in which the square-planar coordination sphere of the cobalt(I) is probably very similar to that shown in Figure 1 for $Co^{I}L_3^{+}$. However, there is reason to suspect that the situation may differ for the conjugated-diene ligands L_1 and L_2. It is known that[34a] one-electron reduction yields the bound radical $Ni^{II}(L^{-})^{+}$ for NiL_1^{2+} and NiL_2^{2+} and that[34b] $Ni^{II}(L_1^{-})^{+}$ radical dimerizes to form diamagnetic adducts in solution.[34b] The spectra of $Ni^{II}(L_1^{-})^{+}$ monomer and CoL_1^{+} are quite similar despite the differing assignments[34] of the reduction sites in these complexes. The spectra of $Ni^{II}(L_2^{-})^{+}$ radical and CoL_2^{+} are quite similar, but strikingly different from those of the other $Co^{I}L_1^{+}$ species. In metal-centered reduction processes, the nickel complexes exhibit more positive $M^{II/I}$ reduction potentials than the corresponding cobalt complexes.[34a,b] Since the reduction potentials for the cobalt(II) complexes of L_1 and L_2 are 0 to 100 mV more positive than those of the corresponding nickel(II) complexes, ligand-centered reduction would be expected in these cobalt complexes. Unfortunately, there is no independent evidence bearing on this issue (for example, dimerization of the CoL^{+} species as found for NiL_1^{+} in CH_3CN) and the comparison of the reduction potentials discussed above may be complicated because $Ni^{II}L_1^{2+}$ and $Ni^{II}L_2^{2+}$ are high spin and the corresponding cobalt complexes are low spin in CH_3CN. It should also be mentioned that an unusual Lewis acid role for CoL_1^{+} has been reported by Kildahl et al.[34c]

As was also found by Tait et al.,[29] the reduction potentials for the $Co^{II/I}$ couple (Table VII) vary in a manner related to ligand unsaturation; the tetraene complex $Co^{I}L_1^{+}$ is the weakest reductant, while the monoene $Co^{I}L_8^{+}$ is the strongest. Interestingly, for L_3, L_5, and L_7, which differ only in the number of methyl group substituents, the order of reduction potentials is opposite that expected from the electron-donating nature of methyl groups. This unexpected pattern has also been observed[29,34] for the reduction potentials ($M^{III/II}$ and $M^{II/I}$) of Ni, Co, and Cu complexes of Me_2[14]ane, Me_4[14]ane, Me_6[14]ane, L_3, and L_5 and appears to reflect perturbations in the axial ligand fields of the complexes arising from steric interference by the methyl groups. Since the magnitude of the effect is always greater for the higher oxidation state of the metal, the reduction potential drops as the steric interference decreases (higher oxidation state is stabilized).

Because of the reactivity of Co(I) complexes toward O_2 and H_2O, only a few spectra have been reported.[35,36] The spectra we measured (Table V) are similar to those except for small differences in λ_{max} and ϵ, likely due to the different solvents used. All of the cobalt(I) macrocycles (except CoL_2^{+}, see above) are intensely colored, presumably due to metal-to-ligand charge-transfer transitions involving promotion of the metal d (d_{xz}, d_{yz}) electrons to the ligand imine molecular orbitals. The spectra of $Co^{I}L_3^{+}$, $Co^{I}L_5^{+}$, and $Co^{I}L_7^{+}$, in which the macrocycle differs only in the number of positions substituted by methyl groups, are quite similar, having very intense bands at 685, 678, and 658 nm, respectively. If the long-wavelength transitions were purely MLCT in character, they would be expected to shift in the opposite way with metal redox potential. The trend observed is consistent with rather extensive back-bonding between d_{xz} and d_{yz} and the ligand imine functions. The spectrum of $Co^{I}L_5^{+}$ exhibits some solvent dependence, roughly paralleling solvent acceptor number;[37] λ_{max} is 640 nm in H_2O,[36] 678 nm in CH_3CN,[10,35] 686 nm in 28% pyridine in CH_3CN (by volume), and 695 nm in DMF.[10] This trend contrasts with that found for the MLCT bands of ruthenium ammines,[38] for which the interaction of the ammine N–H groups with the solvent molecules leads to a correlation with solvent donor number. Instead, it is reminiscent of the behavior observed for cyano–iron complexes,[39] which is dominated by the interaction

(33) Wishart, J. F. Private communication.
(34) (a) Lovecchio, F. V.; Gore, E. S.; Busch, D. H. *J. Am. Chem. Soc.* **1974**, *96*, 3109. (b) Furenlid, L. R.; Renner, M. W.; Szalda, D. J.; Fujita, E. *J. Am. Chem. Soc.* In press. (c) Kildahl, N. K.; Viriyanon, P. *Inorg. Chem.* **1987**, *26*, 4188.
(35) Vasilevskis, J.; Olson, D. C. *Inorg. Chem.* **1971**, *10*, 1228.
(36) Tait, A. M.; Hoffman, M. Z.; Hayon, E. *J. Am. Chem. Soc.* **1976**, *98*, 86.
(37) Mayer, U.; Gutmann, V.; Gerger, W. *Monatsh. Chem.* **1975**, *106*, 1235.
(38) Creutz, C.; Chou, M. H. *Inorg. Chem.* **1987**, *26*, 2995 and references cited therein.
(39) Toma, H. E.; Takasugi, M. S. *J. Solution Chem.* **1989**, *18*, 575 and references cited therein.

of lone-pair electrons on the cyanide ligands with the protons of hydrogen-bonding solvents. Possibly this correlation signals some weak interaction of the cobalt(I) d electrons with the solvent.

Carbon Monoxide Complexes. The CO adduct of *N-rac*-$Co^{I}L_5^+$ is square-pyramidal,[12c] with the cobalt 0.57 Å above the plane of the four nitrogens. Carbonyl(6,7,13,14-tetramethyl-1,2,4,5,8,9,11,12-octaazacyclotetradeca-2,5,7,12,14-pentaenato)cobalt(I),[40] $Co^{I}L_9$–CO, is also square-pyramidal, with the cobalt atom 0.4 Å above the plane of four coordinating nitrogens, and has $\nu_{C\equiv O}$ at 1965 cm^{-1}. It is likely that all of the CoL_i–CO^+

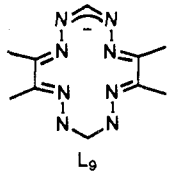

L_9

complexes studied here have a similar square-pyramidal structure. The intensely blue complex $Co^{I}L_1$–CO^+ (which has two sets of conjugated double bonds) and the green complex $Co^{I}L_2$–CO^+ (which has one set) have unusually intense bands at 675 nm; conceivably these transitions are MLCT in character. All of the other CO adducts characterized here are yellow and have similar UV–vis and IR spectroscopic properties and K_{CO} values. For these, the lowest energy band around 1040 nm is evidently a metal-centered (e.g., d_{xy} to $d_{x^2-y^2}$) transition (not unrelated to the lowest energy band observed for $Co^{II}L_5^{2+}$ at 1390 nm), and other d–d transitions may be buried in the tail of the most intense band around 310 nm, which is considered[35] to be a ligand-localized transition. The band around 310 nm is always less intense than that of the corresponding CO_2 adduct.

The relatively large CO binding constants (10^8 M^{-1}) and rather low carbonyl vibrational frequencies (1895–1918 cm^{-1}) of the yellow cobalt(I) carbonyl complexes are consistent with stronger M(I)-to-CO back-donation in these complexes than that in related copper(I)[25b] and nickel(I) CO adducts:[32] for $Cu^{I}L_i$–CO^+ the K_{CO} values are reported[25b] to be $(4.2 \pm 3.0) \times 10^1$ M^{-1} (L_1) and $(4.7 \pm 3.0) \times 10^1$ (L_5) M^{-1} in DMF; for $Ni^{I}L_i$–CO^+, the K_{CO} values are[32] $(1.7 \pm 0.4) \times 10^2$ (L_1), $(1.8 \pm 0.2) \times 10^4$ (L_4), and $(4.7 \pm 0.5) \times 10^4$ (L_5) M^{-1} in DMF and $\nu_{C\equiv O}$ values are 2020, 1957, and 1962 cm^{-1} in pyridine, respectively. In Figure 13, the dependencies of $\nu_{C\equiv O}$ and ln (K_{CO}) on $E_{1/2}$ are shown. As can be seen from this figure, CO stretching frequencies decrease and CO binding constants increase as $Co^{I}L_i^+$ becomes a more powerful reductant. Both trends are consistent with the importance of back-bonding interactions in the binding of CO to cobalt(I). In contrast to the Co^{I}–CO_2^+ complexes (discussed next), in these CO complexes the linear CO ligand seems not to be greatly affected by the amine hydrogen and the methyl group geometry of the macrocycles. In fact, K_{CO} determined by pulse radiolysis for the primary, *N-rac*- (1.6×10^8 M^{-1}) and the *N-meso*-$Co^{I}L_5$ (0.8×10^8 M^{-1}) are quite similar.[12a,b] The slightly larger stability of the primary, N-rac isomer may arise from the square-pyramidal geometry of the complex and the large open space on the secondary face for CO coordination.

Carbon Dioxide Complexes. The CO_2 complexes studied here are 1:1 complexes (see Table IV, Figure 12, and refs 10 and 12) in which the CO_2 is presumably bound η^1-C to an axial metal coordination site[10] (i.e., Co–C(O)O). It appears that, depending on the complex and the conditions, the cobalt center in the CO_2 complex may be either five-coordinate, like the CO adducts discussed above, or six-coordinate, with a solvent molecule or other ligand bound in the axial position trans to the CO_2. As noted earlier, for *N-rac*-L_5 the CO_2 adduct is thermochromic, evidently existing in five-coordinate form at higher temperatures and in six-coordinate form (eq 1) at low temperatures in acetonitrile,[10] butyronitrile,[10] and water.[12a] This interpretation is supported by several lines of evidence: A five-coordinate CoL_5(–C(O)O) moiety is observed in purple crystals of the binuclear $(CoL_5)_2(\mu$-$CO_2H)(ClO_4)_3$.[10] The tan solid collected from a solution of the low-temperature form contains bound acetonitrile. Furthermore, the spectrum of the low-temperature form is similar to that of *trans*-$Co(en)_2(OH_2)(CO_2)^+$, which is known to be six-coordinate,[41] and to the spectra of six-coordinate alkyl $CoL_5(OH_2)R^{2+}$ complexes (R = $-CH_3$, $-C_2H_5$, etc.).[42,43] From the UV–vis spectra of the CO_2 adducts summarized in Table VI the complexes seem to fall into two classes: For L_3, L_4, and L_5, the lowest energy transition occurs at 530–540 nm, with additional bands at 400–460 and 310 nm. In contrast, for L_6, L_7, and L_8, the lowest energy transition is at 450–480 nm. Indeed, the room temperature spectra of the CO_2 adducts of $Co^{I}L_6^+$, $Co^{I}L_7^+$, and $Co^{I}L_8^+$ resemble that of the low-temperature form of $Co^{I}L_5$–CO_2^+ and it is likely that these are also six-coordinate with a solvent molecule as an axial ligand.

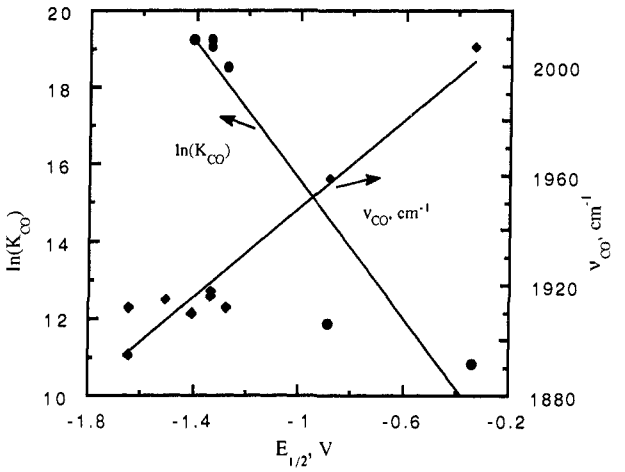

Figure 13. Relationship between $E_{1/2}$ and K_{CO} of $Co^{I}L_i$–CO (i = 1–6) complexes in CH_3CN (left axis) and between $E_{1/2}$ and $\nu_{C\equiv O}$ of $Co^{I}L_i$–CO (i = 1–8) complexes in CH_3CN (right axis).

This coordination number isomerism raises some interesting issues about the nature of these CO_2 complexes: The six-coordinate species such as *trans*-$Co(en)_2(OH_2)(CO_2)^+$ are reasonably regarded as cobalt(III) complexes containing the $-CO_2^{2-}$ ligand and their electronic spectra can be reasonably modeled in terms of ligand-field transitions of cobalt(III).[41] In the six-coordinate complexes, both alkyl and carboxylate ligands labilize the cobalt trans coordination site and lengthen that cobalt–ligand distance.[41,43] Perhaps the five-coordinate form should be considered as the extreme limit of this trans effect. To the extent that charge transfer to the CO_2 is incomplete, substantial metal-d electron density resides along the z axis of the complex, rendering binding of a sixth ligand relatively unfavorable. As charge transfer from the cobalt to the CO_2 increases (as the metal center becomes a more powerful reductant, as with L_6, L_7, and L_8), the electron density along the Co–C axis drops, stabilizing the axial coordination of a trans solvent ligand. Thus the CO_2 complexes of L_3 through L_8 seem to span a considerable range of cobalt-to-CO_2 charge transfer, with the most stable complexes having the greatest cobalt-to-CO_2 charge transfer.

Table VII summarizes $E_{1/2}$ and CO_2 binding constants for these complexes in CH_3CN. Recently Schmidt et al. reported the binding constants in DMSO determined by electrochemical techniques:[13,44] $Co^{I}L_1^+$, $K_{CO_2} < 4$; $Co^{I}L_2^+$, $K_{CO_2} < 4$; Co^{I}[Me_6-[14]1,4,8,11-tetraene]$^+$, $K_{CO_2} < 4$; $Co^{I}L_3^+$, $K_{CO_2} = 7 \pm 5$; *N-meso*-$Co^{I}L_5^+$, $K_{CO_2} = (2.6 \pm 0.5) \times 10^2$; *N-rac*-$Co^{I}L_5^+$, $K_{CO_2} = (3.0 \pm 0.7) \times 10^4$; and $Co^{I}L_6^+$, $K_{CO_2} = (1.0 \pm 0.3) \times 10^5$ M^{-1}.

(40) Goedken, V.; Peng, S.-M. *J. Chem. Soc., Chem. Commun.* **1974**, 914.

(41) Katz, N.; Chou, M. H.; Szalda, D. J.; Creutz, C.; Sutin, N. *J. Am. Chem. Soc.* **1989**, *111*, 6591.

(42) Roche, T. S.; Endicott, J. F. *Inorg. Chem.* **1974**, *13*, 1575.

(43) Endicott, J. F.; Kumar, K.; Schwarz, C. L.; Perkovic, M. W.; Lin, W.-K. *J. Am. Chem. Soc.* **1989**, *111*, 7411.

(44) Schmidt, M. H. Ph.D. Thesis, Stanford University, Stanford, CA, 1989.

Thus the CO_2 binding constants are very similar for DMSO and acetonitrile solvents. The most pronounced trend in Table VII is the correlation between the reduction potentials and the binding constants, and charge transfer from cobalt to CO_2 is an important factor in stabilizing these CO_2 adducts. Only the complexes with $E_{1/2} < -1.2$ V vs SCE in organic solvents bind CO_2 to a detectable degree at room temperature under 1 atm of CO_2. DuBois et al. found[45] such a correlation between $E_{1/2}$ for the second reduction waves of quinones and the CO_2-binding constants (to yield carbonates) in CH_3CN; only quinones that have a second reduction potential more negative than −0.25 V vs SCE bind CO_2.

Although the dependence of K_{CO_2} on reduction potential is pronounced, the data for $Co^IL_4^+$, *N-meso*-$Co^IL_5^+$, and *N-rac*-$Co^IL_5^+$, where the reduction potentials are all −1.34 V vs SCE, implicate additional factors in CO_2 binding. The binding constant for the N-rac isomer of L_5 is about one-hundred times greater than that for the N-meso isomer in CH_3CN, H_2O,[12b] and DMSO.[13,44] For acetonitrile solvent, the equilibrium constant for eq 13 (evaluated from the data in Table VII and for eq 11) is ca.

$$\textit{N-meso}\text{-}Co^IL\text{–}CO_2^+ \rightleftharpoons \textit{N-rac}\text{-}Co^IL\text{–}CO_2^+ \qquad (13)$$

2×10^3. In contrast, the corresponding equilibrium constant for the methyl complex $Co^IL(CH_3)(H_2O)^{2+}$ is only about 5.[43] Several explanations for these differences may be considered: First, as we found in the structure[10] of a CO_2H-bridged cobalt dimer and as Beley et al. suggested in their study[46] of electrocatalytic reduction of CO_2 by Ni(cyclam)$^{2+}$ (cyclam = 1,4,8,11-tetraazatetradecane), an amine hydrogen may interact with an oxygen of CO_2 through hydrogen bonding to provide significant stabilization in addition to that provided by charge transfer from cobalt to CO_2. In the primary, N-rac isomer, CO_2 can interact with both hydrogens of the amine groups, and in the N-meso isomer, CO_2 can make only one hydrogen bond. Second, an axial methyl group in the N-meso isomer may interfere sterically with CO_2 binding. There is no such steric interference in the primary N-rac isomer, where both axial methyl groups are located on the other side of the plane of the four coordinating nitrogens, and a large open space is reserved for CO_2 approach and its binding. (In water, the secondary, N-rac isomer is much less stable than the primary isomer, consistent with both these arguments.[12a]) The behavior of $Co^IL_4^+$, which has a binding constant three-hundred times smaller than *N-rac*-$Co^IL_5^+$, also supports the above argument. Whether $Co^IL_4^+$ is the N-rac or N-meso isomer, CO_2 can interact with only one amine hydrogen. In addition, the cis imine framework of L_4 seems less flexible than the trans imine for attaining stable conformations.

Obviously, N-meso/N-rac isomerism is an important factor for the macrocyclics except CoL_1. More extensive studies should be carried out to assign each isomer and to understand the nature of CO_2 binding.

Finally, we note that, for all cases studied here in acetonitrile solvent, the affinity of the cobalt(I) macrocycle for CO exceeds its affinity for CO_2. This pattern is important to the catalytic reduction of CO_2 to CO because it means that reduction of bound CO_2 to bound CO is thermodynamically more favorable than reduction of free CO_2 to free CO. (Note that for *N-rac*-L_5 in water the opposite is true.[12a])

Concluding Remarks. The series of 14-membered macrocycles used here provide a useful systematic probe of the factors governing the binding of CO and CO_2 to the square-planar, low-spin d^8 cobalt(I) metal center. The CO-binding constants increase from 5×10^4 to $>3 \times 10^8$ M^{-1} as the CoL^{2+}/CoL^+ reduction potential drops from −0.34 to −1.65 V vs SCE; the CO stretching frequencies decrease as the binding constants increase, confirming the importance of back-bonding to the binding. Similarly, charge transfer from cobalt to CO_2 is an important factor in stabilizing the CO_2 adducts. Only the complexes with $E_{1/2} < -1.2$ V vs SCE in organic solvents bind CO_2 to a detectable degree at room temperature under 1 atm of CO_2. However, hydrogen-bonding interactions between the bound CO_2 and amine macrocycle N–H protons may serve to additionally stabilize the adduct in some cases, while steric repulsion by the macrocycle methyl groups may destabilize the adducts, depending upon the complex. Our studies of the CO_2 complexes reveal an extensive isomerism of these macrocyclic CO_2 complexes: conformational, positional, and coordination number isomers enrich the chemistry of these complexes.

Acknowledgment. We thank Drs. B. Brunschwig, S. Feldberg, C. L. Schwarz, H. A. Schwarz, and J. Wishart for helpful discussions, M. Chou for preparing $CoL_3(ClO_4)_2$, and E. Norton for performing analyses for Co, Br^-, Cl^-, and ClO_4^-. We also acknowledge Drs. N. S. Lewis, M. H. Schmidt, and D. L. DuBois for sending their preprints prior to publication. This work was carried out at Brookhaven National Laboratory under contract DE-AC02-76CH00016 with the U.S. Department of Energy and supported by its Division of Chemical Sciences, Office of Basic Energy Sciences.

Supplementary Material Available: Tables of crystallographic data collection parameters, anisotropic thermal parameters for non-hydrogen atoms, non-hydrogen atom positional parameters, calculated hydrogen atom positions, bond distances and angles, and hydrogen-bonding parameters (11 pages); listing of observed and calculated structure factors (7 pages). Ordering information is given on any current masthead page.

(45) DuBois, D. L.; Miedaner, A.; Bell, W.; Smart, J. C. In *Electrochemical and Electrocatalytic Reduction of Carbon Dioxide*; Sullivan, B. P., Ed.; Elsevier: Amsterdam, in press.

(46) Beley, M.; Collin, J. P.; Ruppert, R.; Sauvage, J. P. *J. Am. Chem. Soc.* **1986**, *108*, 7461.